

Molecular-dynamics study of defect formation in *a*-Si:H

Young K. Park and Charles W. Myles

Department of Physics and Engineering Physics, Texas Tech University, Lubbock, Texas 79409-1051

(Received 22 July 1994)

Molecular-dynamics simulations have been performed to investigate the defect formation associated with the Staebler-Wronski (SW) effect in undoped *a*-Si:H and the role that H plays in this process. Semiempirical Si-Si and Si-H total-energy functionals were used to obtain the forces needed for these simulations. Two *a*-Si:H random networks proposed by Guttman and Fong [Phys. Rev. B **26**, 6756 (1982)], a monohydride system and a dihydride system, both of which contain 54 Si and 6 H atoms, were used as initial configurations. The bond-breaking model of the SW effect was assumed, and a localized excitation was used to model the nonradiative energy transfer from photoexcited electron-hole pairs to the system. Our results indicate that the monohydride system is considerably more stable against localized excitations than the dihydride system. We also find that, at least within the bond-breaking model, H is probably not involved in the defect formation associated with the SW effect in undoped *a*-Si:H.

I. INTRODUCTION AND BACKGROUND

Hydrogenated amorphous silicon (*a*-Si:H) is useful in a variety of electronic devices.^{1,2} However, there is a reversible, light-induced, fundamental degradation of this material which limits its device applications. This is known as the "Staebler-Wronski (SW) effect."³ An understanding of the SW effect can have practical importance and is also an interesting basic physics problem. In this paper, we present results of molecular-dynamics (MD) simulations which were performed to investigate this phenomenon and the role of H in the associated defect formation in undoped *a*-Si:H.

The SW effect may be summarized as follows. Prolonged exposure to light of *a*-Si:H films leads to a decrease in the dark conductivity and the photoconductivity. These can be restored by annealing at 150–220 °C in the dark.^{1,2} Metastable midgap defects in *a*-Si:H can be produced by illumination. In the SW effect, it is believed that the nonradiative recombination of photoexcited carriers is responsible for the creation of these defects.⁴ It is also generally accepted that these light-induced defects, commonly believed to be threefold coordinated Si atoms or dangling bonds, are responsible for the conductivity decrease. In order to improve *a*-Si:H device quality, it is essential both to understand the mechanisms and defects responsible for this fundamental instability and to understand the role that H plays in this process.

Several microscopic mechanisms have been proposed to explain the SW effect. Among these, the bond-breaking model^{4–7} has been the most generally accepted. This model is based on the idea that the metastable defects are created by "weak" Si-Si or Si-H bonds being broken by the energy released in the nonradiative recombination of the photoexcited electron-hole pairs. However, a quantum-mechanical description of these weak bonds has not been offered.⁸ It is this bond-breaking model that we utilize in the present paper and that we simulate by the method discussed below.

Within the bond-breaking model, there are at least three variations. In Refs. 5 and 6, it is suggested that the metastable defects are produced simply by the breaking of weak Si-Si bonds with the creation of dangling bonds. On the other hand, Stutzmann, Jackson, and Tsai⁴ proposed that the energy released by the nonradiative recombination of the photoexcited carriers leads not only to the breaking of weak Si-Si bonds and the creation of dangling bonds, but also to the rearrangement of some of the H atoms. Finally, Qin and Kong⁷ proposed a weak Si-H bond-breaking model to explain this effect.

It is possible that H plays an important role in defect formation in the SW effect, and some recent theories⁹ support this idea. However, recent experimental work¹⁰ and other recent theories¹¹ indicate that the light-induced defects in the SW effect are probably not created near H atoms. This casts doubt on theories⁹ which require rearrangement of H's in the defect formation. What role H plays in the SW effect is thus, at present, unclear. One of the purposes of this study is to clarify this issue by investigating the role of H in light-induced defect formation in *a*-Si:H.

Recently, there have been several MD simulations of *a*-Si:H using forces obtained from classical interatomic potentials, whose form is based on physically motivated guesses.^{11,12} By contrast, in the present paper, the forces are obtained from quantum-mechanically-derived total-energy functionals which describe the system more generally.^{13,14} The semiempirical total-energy functionals of Carlsson, Fedders, and Myles¹³ (CFM) and of Park and Myles¹⁴ (PM) are used for the Si-Si and Si-H interactions, respectively. The forms of these tight-binding-based cluster functionals are based on the moment method.¹⁵ Thus, they do not have the form of interatomic potentials. Further, even though they are tight-binding based, they do not have the usual tight-binding form. In particular, these parametrized functionals depend on a tight-binding Hamiltonian which is never diagonalized. Instead, the sum of occupied energy levels is given by an

approximate, *quantum-mechanically-derived*, expression involving the first four moments of the Hamiltonian. The parameters on which these functionals depend are determined by fits to a large database of experimental and theoretical properties of Si and Si-H systems. More details, including the derivations of these functionals, their explicit forms, and the results of their tests on a large number of Si and Si-H systems may be found in Refs. 13 and 14.

Thus far, no computer simulation has come to close to reproducing the realistic laboratory conditions required to generate light-induced defect formation in *a*-Si:H. Experimentally, prolonged illumination, particularly at high light intensities, leads to a saturation of the metastable defect density, with saturated densities of the order 10^{17} cm^{-3} for device-quality films.¹⁶ The SW effect thus occurs with a probability of about 10^{-4} to 10^{-5} per atom. Molecular-dynamics simulations for covalently bonded materials are typically performed with supercells containing less than a few hundred atoms. Even smaller supercells, containing only 60 atoms, are used here. Therefore, because of its very low probability, the true SW effect is not expected to be generated by our approach. Also, because of the necessity to use short-time steps, it is unlikely that anyone will simulate the true SW effect with realistic laboratory conditions in the near future. However, it is still possible to introduce relevant defects that may be connected to the SW effect into the supercells, and this may provide some insight into the microscopic mechanisms responsible for this effect.

The remainder of this paper is organized as follows. As a test of our MD computer code and of our forces, in Sec. II we present the results of an MD simulation of the spectral density of the silicon dimer, Si_2 . In Sec. III, we discuss the monohydride and dihydride supercell models of an *a*-Si:H random network, proposed by Guttman and Fong,¹⁷ which we use as the initial conditions for our simulations. In Sec. IV, we present results of MD simulations of defect formation in *a*-Si:H, within the bond-breaking model of the SW effect. In Sec. V, we present a summary and conclusions.

II. SPECTRAL DENSITY OF Si_2 ; TEST OF MOLECULAR-DYNAMICS CODE

We have developed a MD code using the velocity form of the Verlet algorithm.¹⁸ Our forces are evaluated using the Hellmann-Feynman theorem¹⁹ with the CFM Si-Si and PM Si-H total-energy functionals. These have been thoroughly discussed and tested in Refs. 13 and 14. As a test of our MD code and as another test of the CFM forces, here, we present the results of an MD calculation of the vibrational spectrum of the Si dimer, Si_2 .

For these calculations, the positions and velocities of the two atoms in Si_2 were computed as functions of time under the constraints that the center of mass was held at a fixed position and that the total linear and angular momenta of the molecule were fixed at zero. The time step $\Delta t = 1.8 \times 10^{-16}$ s (0.18 fs) (Ref. 20) was used and a simulation of 10 000 time steps (1.8 ps) was performed to collect a sample for statistics.

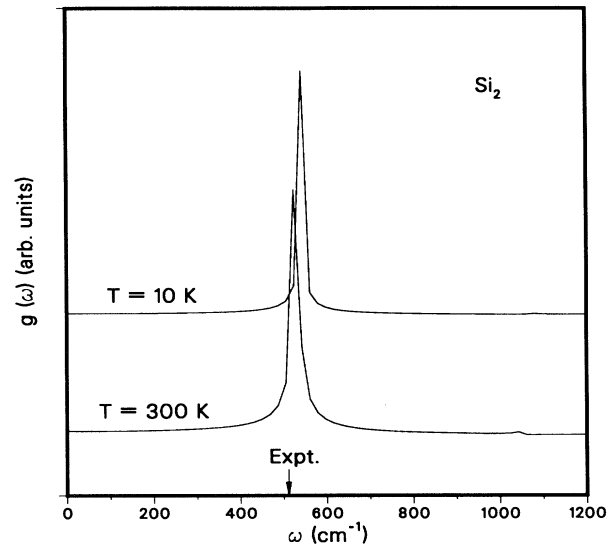


FIG. 1. Vibrational spectral density of Si_2 at $T = 10$ K (upper curve) and 300 K (lower curve), obtained from MD simulations using the CFM forces.¹³ Note the mode softening at high frequencies and the small amplitude, high frequency overtone feature. The peak of the 300-K spectrum is at 524 cm^{-1} . The experimental frequency, 511 cm^{-1} (Ref. 23), is indicated for comparison.

The Fourier cosine transform of the velocity autocorrelation function²¹ was used to compute the spectral density $g(\omega)$,

$$g(\omega) = \frac{\Omega}{2\pi} \int_0^\tau g(t) W(t) \cos(\omega t) dt, \quad (1)$$

where τ is the total time of the simulation, $\Omega = 2\pi/\tau$, $W(t)$ is the Blackman window function²² used to reduce the finite-time sampling oscillations, and $g(t)$ is the velocity autocorrelation function.

In Fig. 1, the results of this calculation are shown for temperatures $T = 10$ K and 300 K. In this figure, the anharmonic effects of mode softening at high excitation levels can clearly be seen. Note that a small amplitude harmonic of the fundamental frequency also appears at high excitation frequencies. The peak of spectrum at 300 K shows a fundamental vibrational frequency of 524 cm^{-1} . This is in very good agreement with the experimental value for Si_2 of 511 cm^{-1} .²³ These results are an indication that our forces and our MD code are both quite reasonable.

III. MODELS OF *a*-Si:H; INITIAL CONDITIONS

Many prescriptions have been given for the construction of realistic models of *a*-Si (Refs. 24–27). Although *a*-Si:H is very important in many applications,^{1,2} due to the difficulties in modeling the Si-H interactions, theoretical models of this material are few in comparison with pure *a*-Si.

For the initial conditions of the simulations reported

here, two *a*-Si:H random network models, a monohydride system and a dihydride system, proposed by Guttman and Fong¹⁷ were used. Both contain 60 atoms; 54 Si and 6 H (≈ 10 at. % H). The optimum material for photovoltaic devices contains 10–15% H.²⁸ The monohydride model, denoted as model 1 in what follows, contains exclusively Si monohydride species and no two H atoms are allowed to be closer than third neighbors. The dihydride model, denoted as model 2 in what follows, contains only Si dihydride species. The coordinates of models 1 and 2 may be found in Tables V and VI, respectively, of Ref. 17, and all Si atom numbers used here are the same as in those tables. The supercell configurations of these models were originally relaxed using a modified Keating potential.¹⁷ Before beginning our simulations, they were further relaxed using the CFM Si-Si and PM Si-H functionals. We have used the supercell method with a 60 atom supercell for models 1 and 2. Periodic boundary conditions were imposed in all directions in a cubic cell. The density of the system was allowed to vary to find the minimum-energy configuration.

The relaxed configuration of model 1 has a mass density $\sim 5.3\%$ smaller than *c*-Si. In this case, all H atoms remained in the monohydride form after relaxation. The average Si-H bond length after relaxation in this model is 1.48 Å and the average Si-Si bond length is 2.37 Å. A notable feature of relaxed model 1 is the absence of coordination defects.

One way to define defects in *a*-Si:H is to say that any Si that is not fourfold coordinated constitutes a defect. Of course, this depends on the definition of a coordination radius or bond cutoff R_0 . However, it is usually accepted that the number of geometrical defects is not highly sensitive to the exact value of R_0 .^{29,30} Small changes in R_0 usually change the relative numbers of dangling bonds and fivefold coordinated floating bonds, without changing the total number of such defects. The detailed values of the bond cutoffs are thus unimportant.²⁹

There were 102 Si-Si bonds and 6 Si-H bonds in the relaxed model 1. Most Si-Si bond lengths were between 2.30 and 2.48 Å. For convenience, we arbitrarily define a normal bond as one with a bond length less than 2.5 Å and a strained bond as one with a bond length between 2.5 and 2.8 Å. A Si-Si pair more than 2.8 Å apart is considered to be broken. The Si-Si bond lengths in model 1 were between 1.45 and 1.52 Å. For convenience, a Si-H pair more than 1.7 Å apart is arbitrarily considered to be broken.³²

The relaxed configuration of model 2 has a mass density $\sim 2.6\%$ smaller than *c*-Si and has one fivefold coordinated defect. In this case, all H atoms remained in the dihydride form after relaxation. The average Si-H bond length after relaxation in this model was 1.41 Å and the average value of the Si-Si bond length was 2.38 Å. The definitions of normal, strained, and broken bonds just discussed were also taken for this case.

Frequently, amorphous materials are characterized by a radial distribution function (RDF), $g(r)$, which measures how atoms organize around one another and which is indicative of local structure. In Fig. 2, we show a comparison of the RDF of models 1 and 2 after relaxation by

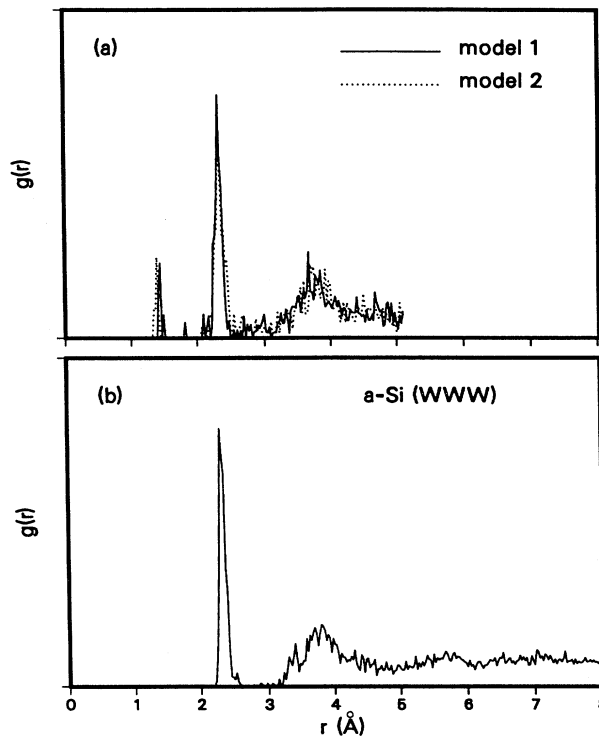


FIG. 2. (a) Radial distribution function (RDF), $g(r)$, for the Guttman and Fong (Ref. 17) model 1 (solid curve) and model 2 (dotted curve), relaxed with the CFM and PM (Refs. 13 and 14) forces. (b) For comparison, the RDF of the 216 atom supercell WWW (Ref. 24) *a*-Si model.

the CFM and PM functionals [Fig. 2(a)] with the RDF of a 216 atom *a*-Si random network proposed by Wooten, and Winer, and Weaire (WWW) (Ref. 24) [Fig. 2(b)]. The first peak, at around 1.48 Å, corresponds to the distance between Si atoms and the nearest H neighbors. The second peak, at around 2.35 Å, corresponds to the nearest-neighbor Si-Si distance. The third peak, at around 4.0 Å, corresponds to the second-neighbor Si-Si distance, which is 3.84 Å in *c*-Si. The much greater width of the third peak of $g(r)$ compared with that for *c*-Si and the shift of this peak from the *c*-Si value show that *a*-Si:H has a distribution of second-neighbor distances, an indication of disorder.

We have also computed the bond angle distributions of the relaxed models 1 and 2 and have compared them with that of the 216 atom WWW *a*-Si model. The agreement is good, once the differences between *a*-Si and *a*-Si:H are accounted for. This distribution is an indication of the fact that the bond angles in *a*-Si:H are not all 109.5° as in *c*-Si. The bond angles after relaxation in both models are distributed between 90° and 130°. The average bond angles are 109.2° and 109.3°, for models 1 and 2, respectively, and the corresponding rms deviations are 10.4° and 9.6°. These are smaller than the 11°–14° of typical computer generated pure *a*-Si networks, such as that of WWW (Ref. 24) and others.^{25–27} This reflects the fact

that, due to the strain relieving role of H, *a*-Si:H has smaller distortions than pure *a*-Si.

IV. MD SIMULATIONS IN *a*-Si:H; THE SW EFFECT

Modeling of the transfer of the recombination energy of an excited electron-hole pair to the *a*-Si:H random network, as in the SW effect, is a difficult problem involving the electron-phonon interaction. A simple, computationally feasible way to do this is to assume that the nonradiative recombination event creates a local excitation (*hot spot*) in the network. We have simulated this by heating the two atoms in a bond with a relatively high excitation energy (usually 2.0 eV). That is, we have given excess kinetic energy to the two atoms which are located at the *hot spot*, which is usually chosen at a weak bond.³¹ In this model, the velocities of the two atoms at this local excitation are assigned in random directions using a pseudorandom number generator. Thus, the *distribution for these random velocities is asymmetric*. This is quite different from the Maxwell-Boltzmann distribution of random velocities assigned as initial conditions in usual MD simulations. In the latter case, the distribution is usually chosen to be symmetric in order to avoid a translational motion of the system as a whole. For both models 1 and 2, we have investigated the effects of a *hot spot* at three types of bonds: (i) weak Si-Si bonds with no neighboring H, (ii) weak Si-Si bonds at hydride sites, and (iii) weak Si-H bonds.

We note that an implicit assumption in our treatment of a *hot spot* is that the electrons are always in their ground states. Thus, the physical effect of bond weakening caused by occupation of antibonding orbitals is not included in our theory. Although such effects have been considered in some *ab initio* theories,⁹ they would be difficult to include within the present tight-binding framework.

Each of our simulations was carried out at an *initial* temperature of 0 K, and involves three major steps. (1) A local excitation energy is applied at a specified bond. (2) The system is allowed to evolve freely without adding or taking away energy. As one intuitively expects, the local disturbance propagates outward and the energy is dissipated shell by shell to the atoms surrounding the *hot spot*. Because of the supercell approximation, after some time, the outgoing energy is reflected at the supercell boundary. This heats the system up and prevents it from reaching true equilibrium. For all excitation energies used, we have found that the disturbance propagates to the supercell boundary in times of the order of ~ 300 fs. Clearly, this time depends on the supercell size (60 atoms in our case). (3) To circumvent this problem, after 300 fs, we quench the system using the power quenching technique.³³ In each simulation, we checked for network structural changes every 100 fs. In some cases, newly generated defects were formed. After quenching, some, but not all, of the newly created defects disappeared. If a defect remained after quenching, we considered it to be a SW effect-related defect. Most of these are dangling bonds and are located at sites where there were initially considerable bond-angle and bond-length distortions.

The forces for these simulations were calculated from the derivative of the total energy, $\mathbf{F} = -\nabla E_{\text{tot}}$. Here E_{tot} is the total energy, which is obtained using the CFM (Ref. 13) and PM (Ref. 14) functionals for Si-Si and Si-H interactions, respectively. The equations of motion for each atom, $\mathbf{F} = m(d^2\mathbf{r}/dt^2)$ (where \mathbf{r} is the atomic position at time t and m is the atomic mass) were solved using the velocity form of the Verlet algorithm¹⁸ with time step $\Delta t = 1.8 \times 10^{-16}$ s (0.18 fs).

As another test of our forces and as tests of both our MD code and our local excitation model, before *a*-Si:H was simulated, the stability of *c*-Si against local excitations was tested. To do this, local excitations of 2.0 to 5.0 eV were applied to various bonds in a *c*-Si supercell with 216 atoms. In all cases, the lattice showed no structural changes after several hundred femtoseconds. This is another indication that our forces are reasonable for Si.

A. Model 1: monohydride system

In Fig. 3, we show typical results of our MD simulations of the effect of a local excitation on the relaxed silicon monohydride model 1. Results for the post-excitation time dependence of the bond lengths for weak Si-Si bonds with no neighboring H, for a weak Si-Si bond at a monohydride site, and for a weak Si-H bond are shown, respectively, in Figs. 3(a), 3(b), and 3(c).

Figure 3(a) shows bond length versus time results for three Si-Si bonds which have no neighboring H. Bonds 19–29 (dotted curve) and 34–51 (dashed curve) are weak bonds with considerable initial strain. Their initial bond lengths were 2.49 and 2.48 Å, respectively, which are longer than most other Si-Si bonds of this type in model 1. For comparison, in Fig. 3(a) we also show results for bond 12–43 (solid curve), which is a typical normal bond with initial bond length 2.29 Å. In all three cases, the excitation was created by heating the bond with an energy of 2.0 eV.

Figure 3(a) shows that the bond lengths oscillate during the 300 fs that the system is allowed to evolve freely. Atom 19 was initially the most weakly bound site in model 1, with an initial site energy of $E_s = -4.24$ eV. This is higher than the average site energy of -4.49 eV for model 1 ($E_s = -4.72$ eV for *c*-Si). Bond 19–29 was the weakest Si-Si bond in model 1. However, from Fig. 3(a) it can be seen that the bond length of this pair fluctuates only by a small amount during the first 300 fs of the simulation and that the excitation does not create a defect. It can also be seen that the same is true of bonds 12–43 and 34–51; none of the three bonds is broken during that time. Since, after ~ 300 fs the disturbance has propagated to the supercell boundary, we quenched the system after that time.³³ As can also be seen in Fig. 3(a) for $t \geq 300$ fs, no essential changes in the bond lengths were caused by this quenching. Similar results were also found for other weak Si-Si bonds with no neighboring H.

In order to examine the role of H in the defect formation associated with the SW effect, local excitations were also simulated at several weak Si-Si bonds on monohydride sites in model 1. In Fig. 3(b), the post-excitation time dependence of the Si-Si bond length is shown for a

typical weak Si-Si bond, bond 40–45 (solid curve). Atom 40 was initially a monohydride site with bond length 2.41 Å. The excitation was created by heating this bond with an energy of 2.0 eV. As can be seen, the bond length oscillated for 300 fs, after which we quenched the system.³³ With the quench, this distance was stretched to 2.51 Å. Thus, after this time, the bond is still quite strained, but is clearly not broken. We also monitored the time dependence of the distance between Si atom 40 and its neighboring H. This is shown as the dotted curve in Fig. 3(b). The initial Si-H bond length was 1.48 Å. As can be seen from the figure, after the excitation, this distance initially shows quite large amplitude oscillations which decrease with time. After the system is quenched, this bond is

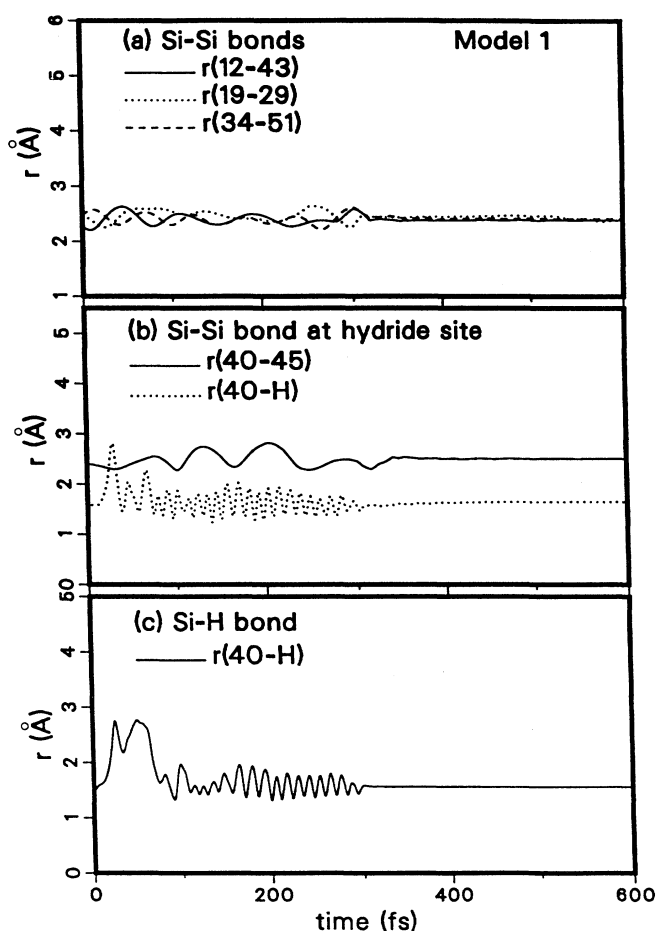


FIG. 3. Molecular-dynamics results, in model 1, for the post-excitation time dependence of the bond length in various bonds to which a local excitation of 2.0 eV has been applied. (a) Results for three weak Si-Si bonds with no neighboring H; bonds 12–43 (solid curve), 19–29 (dotted curve), and 34–51 (dashed curve). (b) Results for a weak Si-Si bond, bond 40–45 (solid curve), at a monohydride site. Results in this same case for the Si-H bond at site 40 are also shown (dotted curve). (c) Results for the weak Si-H bond at site 40. The system was allowed to evolve freely for 300 fs, after which it was quenched (Ref. 33). The time step was 0.18 fs. All Si atom numbers are the same as in Table V of Ref. 17.

stretched to 1.63 Å, but is clearly not broken. Thus, the local excitation clearly neither broke weak Si-Si bond 40–45 nor caused a rearrangement of the H atom at monohydride site 40. However, both the Si-Si and Si-H bonds at site 40 became highly strained after excitation. Similar results were also found for other bonds at monohydride sites.

To examine the possibility of Si-H bond-breaking by a local excitation, simulations were also performed of the effect of a *hot spot* at weak Si-H bonds in model 1. Figure 3(c) illustrates the results of a typical simulation of this. The post-excitation time dependence of the Si-H bond length at site 40 is shown. The initial bond length was 1.48 Å, and an excitation of 2.0 eV was applied. As can be seen, this energy broke the bond at early times. However, this bond eventually healed after around 300 fs as the system was equilibrated. After that time, we quenched the system.³³ As can be seen, the net effect of the local excitation was to stretch the bond to 1.56 Å, but the bond clearly was not permanently broken.

On the basis of these simulations, we conclude that the monohydride model 1 of an *a*-Si:H random network, with ~ 10 at. % H and no coordination defects, is very stable against local excitations, at least at energies ≤ 2.0 eV. We again note that our treatment has neglected the possibility of electronic excitations at the *hot spot*. It is possible that the inclusion of such effects might alter these results. We also note that the bond breaking process may be a low-probability event, so that there might be difficulty observing it with a finite number of simulations.

B. Model 2: dihydride system

Typical results of our MD simulations of the effect of a *hot spot* on the relaxed silicon dihydride model 2 are shown in Figs. 4–7. Results for Si-Si bonds with no bonded neighboring H are shown in Figs. 4 and 5, those for weak Si-Si bonds at a dihydride site are shown in Fig. 7(a), and those for a weak Si-H bond are shown in Fig. 7(b). Figure 6 is a schematic illustration of bond breaking and defect formation caused by a local excitation. In all cases, the system was quenched³³ after 300 fs.

As Si-Si bonds which have no neighboring H atoms, bonds 1–38, 10–17, 40–45, 19–32, and 42–48 were selected for study. These are representative of normal bonds (bonds 1–38, 10–17, and 40–45, with bond lengths ≤ 2.5 Å), and weak bonds (bonds 19–32 and 42–48, with bond lengths ≥ 2.5 Å and considerable initial strain). Localized excitations were created by heating the Si atoms in these bonds.

Figure 4(a) shows typical results of our MD simulations for the normal bonds 1–38 (solid curve), 10–17 (dotted curve), and 40–45 (dashed curve), obtained with an excitation of 2.0 eV. In that figure, the post-excitation time dependences of the bond lengths of these three bonds are shown. As can be seen, the *hot spot* does not break the bond for any of these cases. In order to test the stability of such bonds against a local excitation, an excitation of 5.0 eV was also applied to each of the bonds of Fig. 4(a). The results of our simulation of this applied to bond 40–45 are shown in Fig. 4(b), which shows the

post-excitation time dependence of the bond length of this bond after the 5.0-eV excitation (dotted curve) and after the 2.0-eV excitation (solid curve). As can be seen, the 5.0-eV excitation does not break the bond either. Further, after equilibration by quenching,³³ no essential change is found for the 5.0-eV case, in comparison with the 2.0-eV results.

It is also interesting to monitor the kinetic energy at the *hot spot* as a function of time. Figure 4(c) shows this for bond 40–45 for the 2.0-eV (solid curve) and 5.0-eV (dotted curve) excitations. As can be seen, most of the initial kinetic energy dissipates in ~ 300 fs and the kinetic energy becomes very small after quenching. We, therefore, conclude that these normal bonds in model 2 are very stable against local excitations.

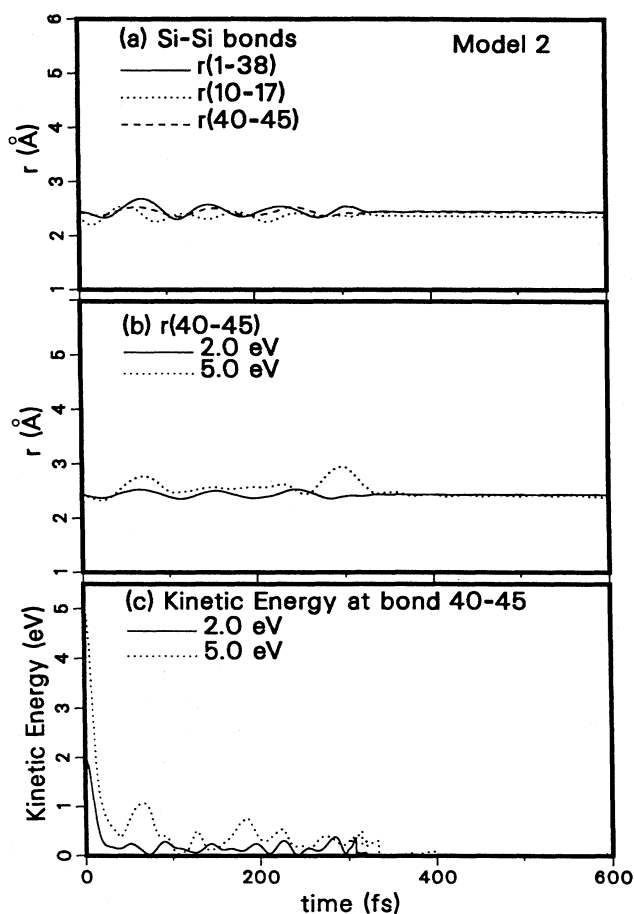


FIG. 4. Molecular-dynamics results, in model 2, for a local excitation applied to Si-Si bonds with no bonded H. (a) Post-excitation time dependence of the bond length in three normal bonds to which a local excitation of 2.0 eV has been applied; bonds 1–38 (solid curve), 10–17 (dotted curve), and 40–45 (dashed curve). (b) Post-excitation time dependence of the bond length in bond 40–45 for two different excitation energies; 2.0 eV (solid curve) and 5.0 eV (dashed curve). (c) Post-excitation time dependence of the local kinetic energy at the *hot spot* for the same cases as in (b); 2.0 eV (solid curve) and 5.0 eV (dashed curve). All atom numbers are the same as in Table VI of Ref. 17. The remainder of the interpretation is the same as in Fig. 3.

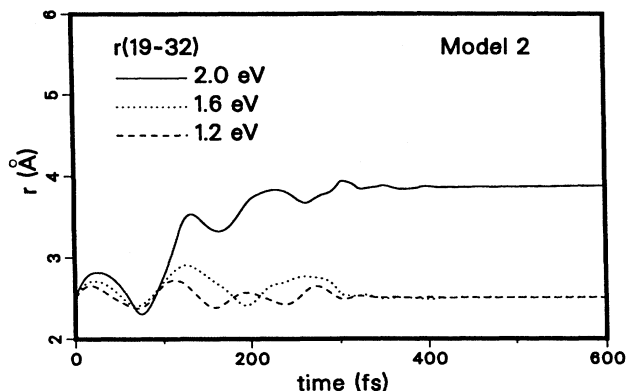


FIG. 5. Molecular-dynamics results, in model 2, for the post-excitation time dependence of the bond length in weak Si-Si bond 19–32, which has no bonded H and to which a local excitation has been applied. Results for three excitation energies are shown: 1.2 eV (dashed curve), 1.6 eV (dotted curve), and 2.0 eV (solid curve). This bond was clearly broken by the 2.0 eV excitation. The remainder of the interpretation is as in Fig. 4.

Typical results of the application of localized excitations in model 2 to weak Si-Si bonds with high initial strain and no neighboring H are illustrated in Fig. 5. This figure shows results of our MD simulations of localized excitations applied to bond 19–32. The post-excitation time dependence of the bond length is shown

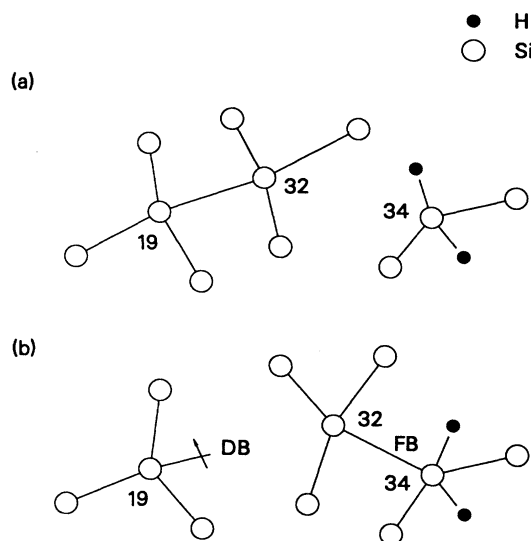


FIG. 6. Schematic illustration (not to scale) of the breaking of weak Si-Si bond 19–32, in model 2, by a local excitation, as in the 2.0-eV case of Fig. 5. Note that this is a two-dimensional schematic of a three-dimensional process. (a) Initial configuration. The initial length of bond 19–32 and the initial bond angles at sites 19 and 32 are highly strained. (b) Final configuration. After bond 19–32 is broken, the local configuration is changed; atom 19 now has a dangling bond and atom 32 is now bonded to atom 34. The new bond 32–34 is highly strained floating bond. The atom numbers are the same as in Table VI of Ref. 17.

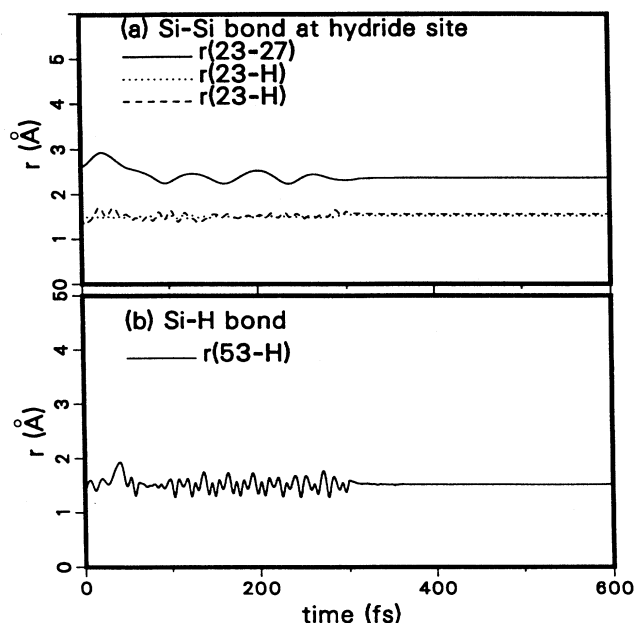


FIG. 7. Molecular-dynamics results, in model 2, for the post-excitation time dependence of the bond lengths for various bonds to which a local excitation of 2.0 eV has been applied. (a) Results for weak Si-Si bond 23–27 (solid curve). Results for the two Si-H bonds at dihydride site 23 are also shown (dotted and dashed curves). (b) Results for the weak Si-H bond at site 53. The remainder of the interpretation is as in Fig. 4.

for three different local excitation energies; 1.2 eV (dashed curve), 1.6 eV (dotted curve), and 2.0 eV (solid curve). The variation in the results with excitation energy is a crude method of modeling the dependence of the SW effect on photon energy. The initial bond length was 2.51 Å and the bond angles were highly distorted. As can be seen, an excitation energy of 2.0 eV breaks the bond after ~ 100 fs. After 300 fs, when we quenched the system,³³ the distance between the two locally excited atoms 19 and 32 was larger than 4.0 Å. There is clearly a threshold energy for this bond breaking. As can be seen in Fig. 5, the 1.2-eV and 1.6-eV excitations fail to break the bond. We have found that the threshold energy for bond breaking in this case is slightly below 2.0 eV, which is much higher than the experimental value of ~ 1.2 – 1.3 eV.³⁴ We note that, experimentally, the threshold energy may vary with the sample condition. The fact that model 2 has only a few strained bonds may help to explain a higher threshold energy than the experimental value.

When a bond is broken after application of a local excitation, other structural changes also occur and defects other than a dangling bond may be created. For bond 19–32, the resulting configuration near the *hot spot* after bond breaking by the 2.0-eV excitation is illustrated schematically in Fig. 6. The initial and final configurations are shown in Figs. 6(a) and 6(b), respectively. A bond has formed between atoms 32 and 34 so that atom 34 has become fivefold coordinated. Therefore, in this case, bond breaking by a localized excitation re-

sults in the creation of a threefold coordinated Si (dangling bond), atom 19, and a fivefold coordinated Si (floating bond), atom 34.

We have found similar results for bond 42–48 in model 2. Atom 48 was the only initially fivefold coordinated site in this model and bond 42–48 was initially highly strained with bond length 2.58 Å. A local excitation of 2.0 eV was applied. Similar to the results shown in Fig. 5, the bond was stretched immediately and broken in ~ 100 fs. This resulted in the fivefold coordinated defect at atom 48 being annihilated and in a threefold coordinated dangling bond being created at atom 42.

Weak Si-Si bonds on dihydride sites were also tested for stability against local excitations. As an example, the results of the application of a 2.0-eV excitation to bond 23–27 are illustrated in Fig. 7(a), which shows the post-excitation time dependence of the Si-Si distance for this bond (solid curve). As can be seen, the excitation did not break the bond. The initial bond length was 2.6 Å. After equilibration by quenching,³³ this bond length became ~ 2.36 Å. Thus, in this case, the excitation relieved much of the strain. In Fig. 7(a), the post-excitation time dependences of the bond lengths between the dihydride-site Si, atom 23, and the two neighboring H atoms are also shown for this case (dashed and dotted curves). The initial Si-H bond lengths were 1.49 and 1.46 Å. As can be seen, after equilibration, these stretched to 1.52 and 1.56 Å.

Finally, the effect of localized excitations on weak Si-H bonds at dihydride sites were also investigated in model 2. Typical results for this case are shown in Fig. 7(b), which illustrates the post excitation time dependence of the Si-H bond length at atom 53 after a 2.0-eV excitation. The initial bond length was 1.41 Å. As can clearly be seen, no bond breaking was produced in this case either. Further, the Si-H bond was stretched to 1.52 Å by this local excitation. Hence, the final configuration is highly strained.

These results indicate that, within model 2 of *a*-Si:H and within the bond-breaking model, defects associated with the SW effect can be created (by excitations of energy ≤ 2.0 eV which leave the electrons in their ground states) only at Si-Si bonds with no bonded H and only at such bonds which are initially highly strained. Also, when a local excitation breaks such a bond, other structural changes, such as the creation of a fivefold coordinated floating bond, can occur.

V. SUMMARY AND CONCLUSIONS

Molecular-dynamics simulations have been performed to try to understand the defect formation associated with the SW effect in undoped *a*-Si:H. The CFM and PM total-energy functionals^{13,14} were used to model the interatomic interactions. These low-order moment schemes, which involve an approximate treatment of the quantum-mechanical electronic total energy, are less accurate than fully quantum-mechanical theories. However, MD simulations based on them, such as those presented here, use much less computational time than *ab initio* theories. Thus, insight into the trends in various proper-

ties from one system to another can be more easily obtained with these schemes.

In these studies, the bond-breaking model of the SW effect was assumed and a localized excitation (*hot spot*) was used to simulate the interaction of the photon with the *a*-Si:H random network. The monohydride (model 1) and dihydride (model 2) *a*-Si:H network models of Guttman and Fong¹⁷ were used as initial conditions. Both models contain 54 Si atoms and 6 H atoms. The supercell approximation with a 60 atom supercell was used in all simulations.

We find that Si monohydride model 1 is very stable against local excitations up to 2.0 eV. By contrast, we find that such local excitations can break bonds in Si dihydride model 2. A threefold coordinated dangling bond can be created by such an excitation and the subsequent rearrangement of the atoms near the *hot spot* can result in the creation of other defects as well. These defects are associated with the SW effect in our model. We find also that these defects can be created only at initially highly strained (weak) Si-Si bonds with no neighboring H. An example of this is the breaking of such a weak bond and the creation of a dangling bond, followed by a local atomic rearrangement which results in the creation of a floating bond. We find no bond breaking near H atoms.

Our major conclusions are that the dihydride model 2 is much less stable against local excitations than the monohydride model 1 and that H is probably not involved in the defect formation associated with the SW effect in undoped *a*-Si:H. Experimentally, it is observed that *a*-Si:H samples with more dihydride species are less stable against light-induced degradation than samples with mostly monohydrides.^{35,36} Furthermore, experiments indicate that defects are probably not created near H atoms.¹⁰ (This is also supported by other theories.³⁷) Our results thus qualitatively support these experiments.

A major assumption in this work is that a local excita-

tion can model the nonradiative energy transfer of photoexcited electron-hole pairs to the *a*-Si:H random network. Here, only a single local excitation was used. However, multiple local excitations in the vicinity of a *hot spot* might increase the probability of the bond-breaking process and of the creation of coordination defects. We note that it may not be adequate to simulate *a*-Si:H with the 60 atom supercells used here because of size effects and because of the fact that bond breaking may be a low-probability event. We hope, however, that this study will provide some insight into the microscopic mechanisms responsible for the SW effect. An investigation into this problem using larger supercells and multiple local excitations is planned.

Tanielian, Goodman, and Fritzsche³⁸ and Skumanich, Amer, and Jackson³⁹ have reported clear evidence that, in the SW effect, high doping of *a*-Si:H results in a higher dangling-bond density produced by a given light exposure. Since *a*-Si solar cells rely on highly conductive p^+ and n^+ layers,⁴⁰ further work including doping effects is necessary to complete this study.

ACKNOWLEDGMENTS

We thank P. A. Fedders, S. Gangopadhyay, C. P. Pal-sule, and S. K. Estreicher for many stimulating discussions. We thank S. K. Estreicher for the use of his workstation to perform these simulations. We are grateful to the Ballistic Missile Defense Organization for a grant through the Office of Naval Research (No. N00014-93-1-0518) and to the Robert A. Welch Foundation for a Grant (No. D-1126), both of which partially supported this work. Y.K.P. thanks the Department of Physics, Texas Tech University, for financial support from the Odetta Greer and J. Fred Bucy Endowment for Applied Physics.

¹R. A. Street, *Hydrogenated Amorphous Silicon* (Cambridge University Press, New York, 1991).

²*Semiconductors and Semimetals*, edited by J. I. Pankove (Academic, New York, 1984), Vol. 21.

³D. L. Staebler and C. R. Wronski, *Appl. Phys. Lett.* **31**, 292 (1977).

⁴M. Stutzmann, W. B. Jackson, and C. C. Tsai, *Phys. Rev. B* **32**, 23 (1985); M. Stutzmann, in *Festkorperprobleme (Advances in Solid State Physics)*, edited by P. Grosse (Pergamon, Braunschweig, 1988), Vol. 28, p. 1.

⁵K. Morigaki, I. Hirabayashi, M. Nakayama, S. Nitta, and K. Shimakawa, *Solid State Commun.* **33**, 851 (1980).

⁶J. I. Pankove and J. E. Berkeyheiser, *Appl. Phys. Lett.* **37**, 705 (1980).

⁷G. G. Qin and G. L. Kong, *Solid State Commun.* **71**, 41 (1989); *Philos. Mag. Lett.* **57**, 117 (1988).

⁸A geometrical definition of a weak bond is commonly used; however, an alternative characterization in terms of self-consistent charge densities is possible. See, I. Štich, R. Car, and M. Parrinello, *Phys. Rev. B* **44**, 11 092 (1991).

⁹See, for example, R. Jones and G. M. S. Lister, *Philos. Mag.*

61, 881 (1990). In this paper, self-consistent, local-density functional methods were used to investigate the role of H in light-induced defect formation in *a*-Si:H. It was found that a bond-centered H atom and a Si dangling bond could be created with formation energies of 0.0–3.0 eV, depending on the strain present in the system. We note that, in this reference, all calculations are static, in contrast to the MD simulations of the present paper. We also note that, in this reference, bond-breaking processes which involve the occupation of antibonding states are included. Such effects are neglected in our work.

¹⁰K. Tanaka (unpublished).

¹¹I. Kwon, R. Biswas, and C. M. Soukoulis, *Phys. Rev. B* **45**, 3332 (1992).

¹²N. Mousseau and L. J. Lewis, *Phys. Rev. B* **43**, 9810 (1991).

¹³A. E. Carlsson, P. A. Fedders, and C. W. Myles, *Phys. Rev. B* **41**, 1247 (1990).

¹⁴Y. K. Park and C. W. Myles, *Phys. Rev. B* **48**, 17 086 (1993).

¹⁵A. E. Carlsson, in *Solid State Physics: Advances in Research and Applications*, edited by D. Turnbull and H. Ehrenreich (Academic, New York, 1990), Vol. 43.

- ¹⁶H. R. Park, J. Z. Liu, and S. Wagner, *Appl. Phys. Lett.* **55**, 2658 (1989).
- ¹⁷L. Guttman and C. Y. Fong, *Phys. Rev. B* **26**, 6756 (1982).
- ¹⁸L. Verlet, *Phys. Rev.* **159**, 98 (1967); D. W. Heermann, *Computer Simulation Methods in Theoretical Physics*, 2nd ed. (Springer-Verlag, New York, 1990); J. M. Haile, *Molecular-Dynamics Simulation* (Wiley, New York, 1992).
- ¹⁹W. Pauli, *Handbuch der Physik* (Springer-Verlag, Berlin, 1933); H. Hellmann, *Einführung in die Quantumchemie* (Franz Deutsche, Leipzig, 1937); R. P. Feynman, *Phys. Rev.* **56**, 340 (1939); B. M. Deb, *Rev. Mod. Phys.* **45**, 22 (1973).
- ²⁰As a rule of thumb, due to the small mass of H, the time step for simulations when H is included is usually chosen to be about $\sim \frac{1}{20}$ of that with only Si. Here, we use the time step appropriate for *a*-Si:H. Therefore, for Si₂, the time step could have been chosen ~ 20 times larger than we used here. To test this fact, MD simulations of Si₂ were performed with several different time steps. The time-dependent motions of the Si atoms along the bond were the same for all time steps ≤ 3.0 fs. However, this was not true for time steps larger than this.
- ²¹O. F. Sankey and D. J. Niklewski, *Phys. Rev. B* **40**, 3979 (1989).
- ²²F. J. Harris, *Proc. IEEE* **66**, 51 (1978).
- ²³M. Menon and K. R. Subbaswamy, *Phys. Rev. B* **47**, 12754 (1993); K. P. Huber and G. Herzberg, *Constants of Diatomic Molecules* (Van Nostrand Reinhold, New York, 1979); S. N. Suchard and J. E. Melzer, *Spectroscopic Data, Homonuclear Diatomic Molecules* (Plenum, New York, 1976), Vol. 2.
- ²⁴F. Wooten, K. Winer, and D. Weaire, *Phys. Rev. Lett.* **54**, 1392 (1985); F. Wooten and D. Weaire, in *Solid State Physics: Advances in Research and Applications*, edited by D. Turnbull and H. Ehrenreich (Academic, New York, 1987), Vol. 40.
- ²⁵J. M. Holender and G. J. Morgan, *J. Phys. Condens. Matter* **3**, 7241 (1991); **4**, 4473 (1992).
- ²⁶W. D. Luedtke and U. Landman, *Phys. Rev. B* **37**, 4656 (1988).
- ²⁷I. Štich, R. Car, and M. Parrinello, *Phys. Rev. B* **44**, 11092 (1991).
- ²⁸L. Guttman, *Phys. Rev. B* **23**, 1866 (1981).
- ²⁹P. A. Fedders, D. A. Drabold, and S. Klemm, *Phys. Rev. B* **45**, 4048 (1992); P. A. Fedders, *J. Non-Cryst. Solids* **137&138**, 141 (1991); D. A. Drabold, J. D. Dow, P. A. Fedders, A. E. Carlsson, and O. F. Sankey, *Phys. Rev. B* **42**, 5345 (1990).
- ³⁰J. M. Holender, G. J. Morgan, and R. Jones, *Phys. Rev. B* **47**, 3991 (1993).
- ³¹We note that there are other methods of simulating a *hot spot*. See, for example, Ref. 9.
- ³²In recent work, the ranges of cutoffs of 2.7–3.0 Å (Refs. 11, 29, and 30) and 1.7–1.74 Å (Refs. 11, 29, and 30) were used to define Si-Si and Si-H bonds, respectively.
- ³³In the technique of *power quenching*, each velocity component is quenched individually. At each time step, if the force and velocity components have opposite sign, the velocity component is set equal to zero. All atoms are then allowed to accelerate at the next time step. This process is repeated until the differences between both the total energies and the forces at the *n*th and the (*n* + 1)st time steps reach a specified tolerance.
- ³⁴Experiment (Ref. 1) shows that for photon energies $\leq \sim 1.2$ eV, no metastable changes in the photoconductivity could be induced even after illumination for longer than 8 h. See also Ref. 4.
- ³⁵V. L. Dalal and C. Fuleihan, in *Amorphous Silicon Technology*, edited by A. Madan, M. J. Thompson, P. C. Taylor, Y. Hamakawa, and P. G. LeComber, MRS Symposia Proceedings No. 149 (Materials Research Society, Pittsburgh, 1989), p. 601.
- ³⁶N. Sakuma, H. Nozaki, T. Niiyama, and H. Ito, in *Amorphous Silicon Technology* (Ref. 35).
- ³⁷P. A. Fedders and A. E. Carlsson, *Phys. Rev. B* **37**, 8506 (1988); P. A. Fedders, Y. Fu, and D. A. Drabold, *Phys. Rev. Lett.* **68**, 1888 (1992).
- ³⁸M. Tanielian, N. Goodman, and H. Fritzsche, *J. Phys. (Paris) Colloq.* **42**, C4-375 (1981), Suppl. 10.
- ³⁹A. Skumanich, N. Amer, and W. Jackson, *Phys. Rev. B* **31**, 2263 (1985).
- ⁴⁰D. E. Carlson and C. R. Wronski, in *Amorphous Semiconductors*, edited by M. H. Brodsky (Springer-Verlag, Berlin, 1979), Chap. 10.